Original Article
The E3 ubiquitin ligase RBCK1 promotes the invasion and metastasis of hepatocellular carcinoma by destroying the PPARγ/PGC1α complex

Zheng Xu[1*], Jun Shao[2*], Cihua Zheng[3*], Jing Cai[4], Bowen Li[2], Xiaogang Peng[5], Leifeng Chen[6], Tiande Liu[2]

*Departments of [1]Head & Neck Surgery, [2]General Surgery, [3]Rehabilitation, Second Affiliated Hospital of Nanchang University, Nanchang 330000, Jiangxi Province, China; [4]Department of Oncology, The Second Affiliated Hospital of Nanchang University, Nanchang 330006, Jiangxi Province, China; [5]Jiangxi Province Key Laboratory of Molecular Medicine, Second Affiliated Hospital of Nanchang University, Nanchang 330000, Jiangxi Province, China; [6]Cancer Center, Renmin Hospital of Wuhan University, Wuhan 430060, Hubei, China. *Equal contributors.*

Abstract: The disruption of tumour cell metabolism can inhibit tumour metastasis, indicating that aerobic glycolysis is central to tumour development. However, the key factors responsible for mediating aerobic glycolysis in hepatocellular carcinoma (HCC) remain unknown. Here, we observed that RBCK1 expression was significantly upregulated in HCC tissues. Our clinical study revealed that high RBCK1 expression is significantly correlated with poor tumour survival and distant invasion. Functional assays revealed that RBCK1 promotes migration and invasion by enhancing GLUT1-mediated aerobic glycolysis. Furthermore, RBCK1-induced HCC cell migration and aerobic glycolysis via activation of WNT/β-catenin/GLUT1 pathway, which was dependent on the destruction of the PPARγ/PGC1α complex. Mechanistically, RBCK1 promotes PPARγ ubiquitination and degradation, and RBCK1 overexpression enhances the transcriptional activity of WNT/β-catenin, thus to upregulate the expression of GLUT1-mediated aerobic glycolysis in HCC cells. Altogether, our findings identify a mechanism used by HCC cells to survive the nutrient-poor tumour microenvironment and provide insight into the role of RBCK1 in HCC cellular adaptation to metabolic stresses.

Keywords: Hepatocellular carcinoma, RBCK, GLUT1, PPARγ/PGC1α complex, metastasis and invasion

Introduction

Aerobic glycolysis, also known as the Warburg effect, is one of the most characteristic metabolic phenotypes of cancer cells, including hepatocellular carcinoma (HCC), where it plays an important role [1, 2]. Aerobic glycolysis is primarily affected by carcinogenic signals, such as PI3K/Akt [3]. It is important to note that a metabolic disorder in tumour cells can inhibit metastasis, indicating that aerobic glycolysis is at the core of tumour growth and survival [4]. Therefore, a better understanding of the mechanisms between cell metabolism and metastasis is essential for the development of new therapies, especially in liver cancer and other diseases, as the liver is an important organ responsible for several unique metabolic functions.

Glucose transporter 1 (GLUT1) belongs to the facilitative cell surface glucose transporter family, the members of which regulate glucose transport across the cell membrane [5]. GLUT1 is overexpressed in several types of cancers [6, 7]. Accumulating evidence suggests that GLUT1 promotes cell proliferation and metastasis, playing a key role in various types of cancer, including HCC [8], breast cancer [9], and kidney cancer [10]. Many studies indicate that the SIRT1/GLUT1 axis promotes bladder cancer progression via regulation of glucose uptake [11]. Furthermore, knocking down GLUT1 in ER-positive breast cancer cell lines rendered cells sensitive to tamoxifen therapy and even restored sensitivity to the drug in tamoxifen-resistant cells [12]. However, the mechanism underlying the regulation of GLUT1-mediated aerobic glycolysis in HCC metastasis remains unclear.

Table 1. Relationship between RBCK1 expression and clinicopathological features

| Parameters | n | RBCK1 expression | | P value |
		Low (n=70)	High (n=146)	
Age (years)				P=0.694
≤65	90	31	59	
>65	126	39	87	
Sex				P=0.363
Female	113	33	80	
Male	103	37	66	
Tumor size (cm)				P=0.164
<5	129	47	82	
≥5	87	23	64	
TNM				P=0.002**
T1-T2	110	47	63	
T3-T4	106	23	83	
Distant metastasis				P=0.013*
No	90	38	52	
YES	126	32	94	
Stage				P=0.006**
I-II	96	41	55	
III-IV	120	29	91	
Differentiation				P=0.173
Well	123	45	78	
Moderate/Poor	93	25	68	

*$P<0.05$, **$P<0.01$.

The ubiquitin-proteasome system (UPS) is an important regulator of cell signalling and proteostasis, both of which are essential for various cellular processes [13]. As one of the most widespread and frequent cellular posttranslational modifications, ubiquitination is also essential for normal cellular functions [14-16]. Posttranslational modification by E3 ubiquitin ligases modulates the functions of target proteins, as well as their fate and intracellular mechanisms [17]. Emerging evidence has identified E3 ubiquitin ligases as a key regulator of cancer. Recently, RANBP2-type and C3HC4-type zinc finger-containing 1 (RBCK1), an E3 ubiquitin ligase with an N-terminal ubiquitin-like (UBL) domain, an Npl4-type zinc finger (NZF) domain and a catalytic C-terminal RBR domain, was shown to have important roles in cancer development [18]. Growing evidence indicates that RBCK1 is involved in immune regulation, antiviral signalling, iron and xenobiotic metabolism, and cancer [19]. RBCK1 can directly interact with numerous proteins implicated in an extensive range of cellular processes, including the cell cycle and transcription.

For instance, Liu et al. [20] demonstrated that RBCK1 modulates chemosensitivity in colorectal cancer (CRC) and may serve as a promising therapeutic target for CRC prevention. Yu et al. [21] demonstrated that RBCK1 is overexpressed in human renal cell carcinoma, highlighting its potential as a therapeutic target for human cancers. RBCK1 also promotes the progression of lung adenocarcinoma by destabilizing the tumour suppressor PKCζ [22]. Furthermore, RBCK1 mRNA levels have been found to be elevated in HCC tissues in both The Cancer Genome Atlas (TCGA) and GSE datasets. These findings suggest that RBCK1 may play an important role in HCC tumorigenesis and development. However, the precise role and underlying signalling cascade of RBCK1 in the progression of HCC remain unclear.

In this study, we first demonstrated that high RBCK1 expression levels were associated with poor prognosis in patients with HCC and revealed the molecular mechanism of RBCK1 in the metabolism and progression of HCC. RBCK1 promotes HCC cell metastasis by enhancing the Warburg effect via GLUT1, and the mechanism underlying RBCK1-mediated regulation of WNT/β-catenin/GLUT1 pathway-induced HCC cell migration and aerobic glycolysis is dependent on destruction of the PPARγ/PGC1α complex. Collectively, our data suggest that RBCK1 may represent a new candidate therapeutic target in HCC.

Methods

Patients and specimens

Cancerous and noncancerous tissues were obtained from 216 patients with primary liver cancer at the Department of General Surgery, the Second Affiliated Hospital of Nanchang University. Pathologists confirmed that all specimens were from normal tissues. This study was approved by the clinical research ethics committee of the Second Affiliated Hospital of Nanchang University, and all subjects agreed to provide samples for research purposes. **Table 1** summarizes the clinical characteristics of all patients.

Cell lines and culture

Four HCC cell lines (HCCLM3, Hep3B, SMMC-7721 and MHCC97H) and normal human he-

patocytes (HL-7702) were obtained from Rockville, USA. The cells were cultured in RPMI 1640 or DMEM (Gibco) supplemented with 10% FBS, 100 U mL^{-1} penicillin, and 100 mg mL^{-1} streptomycin at 37°C and 5% CO_2.

Western blot analysis

Cell lysates were separated using 4-12% Bis-Tris gels (Life Technologies, USA) and transferred to PVDF membranes. The membranes were sealed with 5% skimmed milk in TBST buffer and incubated with the corresponding antibody. The antibodies used were anti-RBCK1 (1:1000, Abcam, ab219955), anti-GLUT1 (1:1000, Abcam, ab115730), anti-PPARγ (1:1000, Abcam, ab45036), anti-PGC1α (1:1000, Abcam, ab176328), anti-β-catenin (1:1000, Abcam, ab16051), anti-UB (1:1000, Abcam, ab134953), anti-UBE1 (1:1000, Proteintech, 15912-1-AP), anti-UBCH5C (1:1000, Proteintech, 11677-1-AP), anti-FBXO9 (1:1000, Proteintech, 11161-1-AP), and anti-tubulin (1:1000, Santa Cruz, sc-8035).

Immunohistochemical (IHC) staining

HCC tissues were fixed, embedded, sectioned, and deparaffinized. A few of the dewaxed sections were subjected to haematoxylin and eosin (H&E) staining. IHC staining was performed according to the manufacturer's instructions using the Dako EnVision™ system (Agilent Technologies, USA). The cells were incubated with anti-RBCK1 (1:200, Abcam, ab219955), anti-GLUT1 (1:200, Abcam, ab115730), anti-PPARγ (1:200, Abcam, ab45036), anti-PGC1α (1:200, Abcam, ab191838), anti-β-catenin (1:200, Abcam, ab16051), anti-Vimentin (1:200, Abcam, ab92547) and anti-Ki67 (1:200, Proteintech, 27309-1-AP) and for 30 min.

shRNA plasmids and constructs

shRNA-mediated double stranded RNA (shRNA) silencing RBCK1 (shRBCK1), β-catenin (shβ-catenin), or GLUT1 (shGLUT1) was synthesized by a gene pharmaceutical company in Shanghai, China. The full-length cDNA of human RBCK1, β-catenin, or GLUT1 was synthesized using gene pharmaceutical technologies and ligated to the pcDNA3.1 vector to generate p-RBCK1, p-β-catenin, or p-GLUT1 marked by flag tag, respectively. A blank vector was used as a negative control. These shRNA plasmids

and constructs were transfected using Lipofectamine 2000 transfection reagent (Invitrogen, USA) according to the manufacturer's instructions.

Cell migration and invasion assays

Transwell assays were routinely used to assess the migration and invasion of HCC cell lines, with a few modifications [23]. For cell invasion assays, a layer of matrix gel was precoated on the upper part of the polycarbonate membrane.

In vivo metastasis assay

For *in vivo* metastasis assays, $1×10^6$ cells in 100 µL of phosphate-buffered saline were injected subcutaneously into the flanks of nude mice. Once the subcutaneous tumours reached 1 to 2 cm in diameter, they were removed and cut into pieces with a volume of approximately 1 mm^3, and then the pieces were implanted into the livers of the nude mice (8 in each group, male BALB/c-nu/nu, 6-8 weeks old). The mice were sacrificed 6 weeks after tumour implantation. The livers and lungs were then processed and embedded in paraffin. The animal work was approved by the animal experimental ethics committee of the Second Affiliated Hospital of Nanchang University and was performed according to the Guide for the Care and Use of Experimental Animals.

Determination of the oxygen consumption rate (OCR) and extracellular acidification rate (ECAR)

The Extracellular Flux Analyser XF96 (Seahorse Bioscience, Billerica, MA, USA) was employed to measure cellular glycolysis capacity and cellular mitochondrial respiration using the XF Cell Mito Stress Test Kit and Glycolysis Stress Test Kit (Seahorse Bioscience), respectively, according to the manufacturer's instructions.

Co-immunoprecipitation (Co-IP) and ubiquitination assays

Immunoprecipitation analysis was performed as previously described. For *in vivo* ubiquitination experiments, the HA-ubiquitin plasmid was stably transfected into RBCK1-knockdown human hepatoma cells or control cells. Two days after transfection, cells were treated with 10 mmol L^{-1} MG132 for 10 h to prevent protea-

some degradation. The lysate was extracted using 2 mg of HA-tagged or IgG antibody. The eluent was separated by SDS-PAGE, and Western blotting was performed using antibodies against RBCK1, PPARγ, and tubulin. For *in vitro* ubiquitination assays, the standard reaction mixture (25 μL) consisted of 20 mM HEPES NaOH (pH 7.5), 50 mM NaCl, 0.02 mg mL^{-1} BSA, 1 mM DTT, 5 mM MgCl$_2$, 1 mM ATP, His-PPARγ (1 pmol as tetramer), E1 (0.85 pmol), UbcH5c (1.25 pmol), FBXO9 (0.8 pmol), and Ub (174 pmol). The reaction mixture was prepared on ice and incubated at 30°C for 10 min unless otherwise specified. SDS buffer was added to terminate the reaction, and Western blotting was performed using PPARγ and tubulin antibodies.

Statistical analysis

All results are shown as the mean ± SD, and at least three independent experiments were analysed using GraphPad Prism 5 software (USA). We used the Kaplan-Meier method to generate survival curves, and the log-rank test was used to assess statistical significance. Differences among groups were analysed using the double tailed t-test and ANOVA. Results were considered statistically significant when P<0.05.

Results

*High expression of RBCK1 is correlated with poor outcomes in HCC patients*

TCGA cohort (n=424) analyses revealed upregulation of RBCK1 in HCC, and high expression of RBCK1 in HCC patients was positively correlated with tumour stage and distant invasion (**Figure 1A-C**). To further determine RBCK1 expression in HCC, qRT-PCR analyses were performed on HCC tissues and their corresponding adjacent tissues. The results showed an average fold change in RBCK1 mRNA expression in HCC tissues compared to adjacent nontumor-bearing tissues (**Figure 1D** and **1E**). Moreover, analysis of the results obtained from Western blotting (**Figure 1F** and **1G**) and IHC staining (**Figure 1H**) revealed that the RBCK1 protein was upregulated in HCC tissues compared to adjacent nontumor-bearing tissues. These results indicate that RBCK1 expression is significantly upregulated in HCC tissues.

Evaluating the correlations between RBCK1 overexpression and HCC clinicopathologic parameters revealed no significant association between RBCK1 expression and tumour size, age or histological type, but a significant correlation with TNM (P=0.002), distant metastasis (P=0.013) and clinical stage (P=0.006) was observed (**Table 1**). Additionally, the 216 HCC patients were divided into two groups based on the results of the immunohistochemical analysis: a high RBCK1 expression group (n=146) and a low RBCK1 expression group (n=70). Kaplan-Meier survival analysis showed that HCC patients with high RBCK1 expression levels exhibited poor overall survival (OS) (P=0.025) and poor disease-free survival (DFS) (P=0.0034) compared to patients with low RBCK1 levels (**Figure 1I** and **1J**). It should be noted that the results of multivariate Cox regression analysis indicated that RBCK1 overexpression was one of the independent predictive factors for poor outcome in HCC patients (**Table 2**). Collectively, these data suggest that RBCK1 is upregulated in HCC tissues and is associated with an unfavourable prognosis in HCC patients.

RBCK1 accelerates the metastasis of HCC cells in vitro and in vivo

To investigate the potential biological function of RBCK1 in HCC development, we first assessed RBCK1 expression in HCC cell lines. qRT-PCR and Western blot results demonstrated that RBCK1 was significantly upregulated in HCC cells compared to the normal HL-7702 cell line (**Figure 2A** and **2B**). Based on the RBCK1 expression levels in HCC cell lines, we next established stable models of RBCK1 knockdown in the HCCLM3 cell line, as well as stable models of RBCK1 overexpression in the Hep3B cell line (**Figure 2C**). Migration and invasion assays revealed that the mobility and invasiveness of HCC cells was markedly inhibited by RBCK1 knockdown but significantly promoted by RBCK1 overexpression compared to control cells (**Figure 2D** and **2E**). Similarly, RTCA assay results also indicated that RBCK1 knockdown notably suppressed the metastatic ability of HCCLM3 cells, while RBCK1 overexpression promoted the metastatic ability of Hep3B cells (Figure S1). As EMT is significantly associated with the metastatic abilities of cancer cells, we examined the effects of RBCK1 expression on
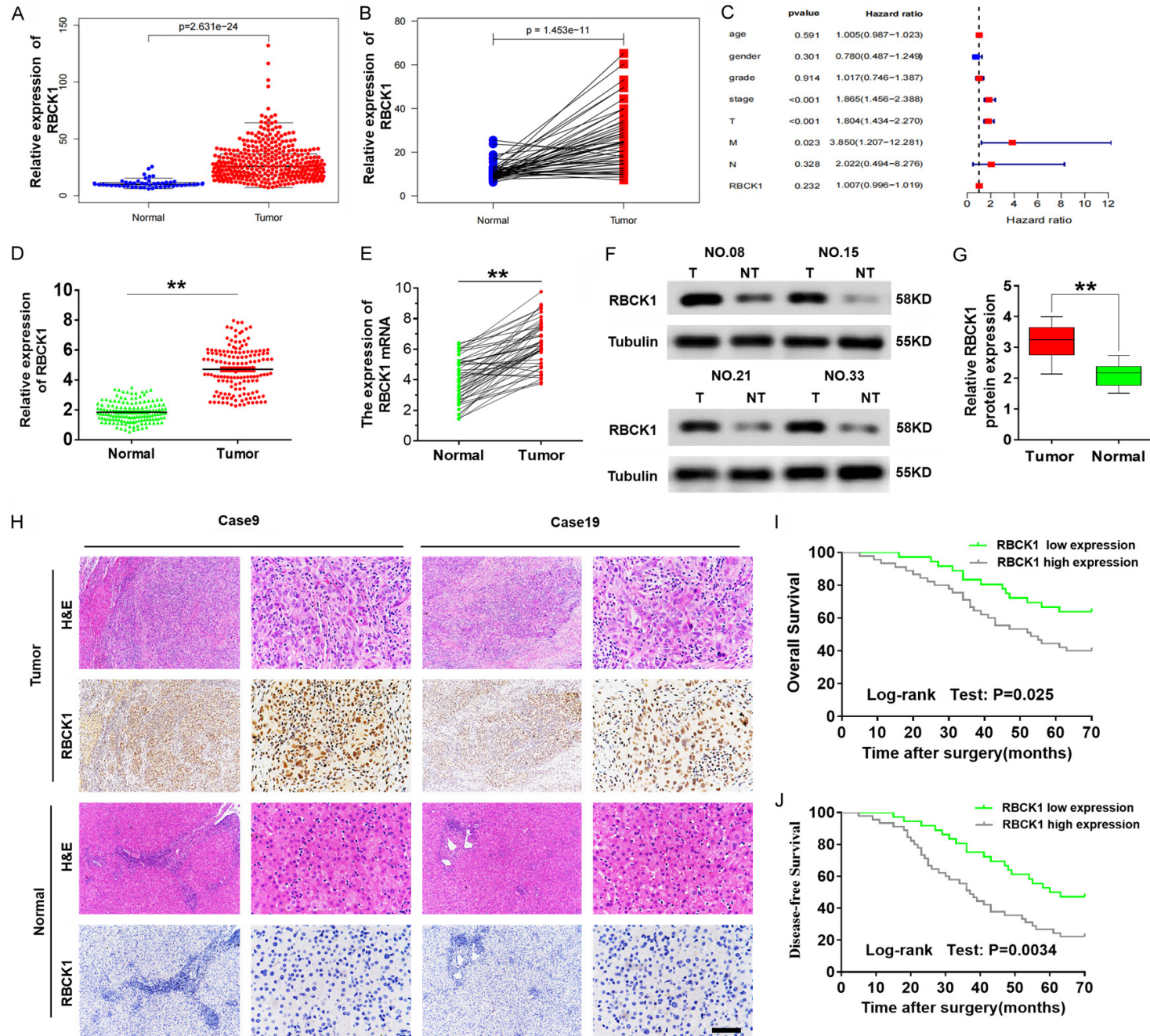
Figure 1. RBCK1 is overexpressed in metastatic HCC and closely correlates with poor prognosis in patients. (A and B) RBCK1 mRNA expression profiles in the TCGA liver cancer dataset. (C) Association with RBCK1 expression and clinicopathological characteristics in HCC patients in the TCGA cohort. (D-G) Expression levels of RBCK1 mRNA and protein in clinical HCC tissues and their adjacent noncarcinoma normal tissues were investigated by qRT-PCR (D and E) and Western blot assay (F and G), respectively. $^{**}P<0.01$. (H) Immunohistochemistry was employed to identify the expression of RBCK1 protein in HCC tissues and their adjacent noncarcinoma normal tissues. Scale bar, 50 μm. (I and J) Kaplan-Meier curves for overall survival (I) and disease-free survival (J) of two groups of HCC patients defined by low and high expression of RBCK1.

Table 2. Univariate and multivariate analyses of overall survival in HCC patients

Parameters	Univariate analysis			Multivariate analysis		
	HR	95%CI	P value	HR	95%CI	P value
Age (≥65 vs <65)	1.437	0.731-2.826	0.736	—	—	—
Sex (Female vs Male)	1.851	0.584-2.927	0.724	—	—	—
Tumor size (>5 vs ≥6)	1.637	1.153-5.176	0.226	—	—	—
Differentiation (Well vs Moderate/Poor)	1.724	1.652-4.16	0.278	—	—	—
TNM stage (T1-T2 vs T3-T4)	2.607	1.415-5.542	0.012*	1.673	1.441-4.534	0.031*
Distant metastasis (No vs Yes)	1.381	0.716-3.765	0.031*	1.721	1.419-2.917	0.089
Stage (I-II vs III-IV)	0.749	0.654-1.867	0.017*	1.432	0.983-3.837	0.037*
RBCK1 expression (High vs Low)	3.847	2.546-5.629	0.001**	2.231	1.736-4.841	0.019*

*P<0.05, **P<0.01.

the EMT phenotype of HCC cells. As shown in **Figure 2F** and **2G**, immunofluorescence assays indicated that RBCK1 knockdown increased epithelial markers and decreased mesenchymal markers in HCCLM3 cells. Therefore, stable RBCK1 knockdown inhibits HCC invasion and metastasis.

We next examined the effects of RBCK1 on HCC metastasis by establishing an orthotopic liver tumour model in nude mice and included shNC and shRBCK1 groups. Histological analysis showed the development of intrahepatic metastasis in five cases from the shNC group compared to only one case in the HCCLM3-shRBCK1 group (**Figure 2H** and **2J**). In addition, H&E-stained serial lung sections revealed that the number of HCC lung micrometastases was significantly decreased in the shRBCK1 group (**Figure 2I**). In contrast, overexpression of RBCK1 increased the number of intrahepatic and lung metastatic nodules (**Figure 2K**). Collectively, these results indicate that stable knockdown of RBCK1 inhibits HCC invasion and metastasis both *in vitro* and *in vivo*, indicating that RBCK1 is a candidate tumour oncogene in HCC progression and metastasis.

RBCK1 promotes HCC progression by enhancing the Warburg effect

E3 ubiquitin ligases contribute to reprogramming metabolism in the progression of several types of cancer. As the Warburg effect is a well-characterised metabolic shift that ubiquitously occurs in tumour cells, including HCC, we explored the role of RBCK1 in HCC glucose metabolism. RBCK1 knockdown also dramatically decreased cellular levels of glucose-6-phosphate (G6P), glucose consumption, lactate production, and ATP in HCCLM3 cells (**Figure 3A**), while RBCK1 overexpression caused the opposite trends in Hep3B cells (**Figure 3F**). To further validate the impact of RBCK1 on glycolysis in HCC, ECAR, which reflects overall glycolytic flux, was measured. RBCK1 knockdown was shown to significantly decrease the glycolytic rate and capacity of HCCLM3 cells (**Figure 3B** and **3C**), whereas RBCK1 overexpression increased the ECAR in Hep3B cells (**Figure 3G** and **3H**). The results obtained from the measurement of OCR, an indicator of mitochondrial respiration, revealed an increase in HCCLM3/shRBCK1 cells (**Figure 3D** and **3E**), whereas RBCK1 overexpression induced a decrease in Hep3B cells (**Figure 3I** and **3J**). Moreover, these respective responses were also observed in MHCC97h/shRBCK1 and SMCC7721/p-RBCK1 cells (Figure S2).

To investigate whether the Warburg effect was responsible for the progression of HCC cells, HCCLM3/shRBCK1 and Hep3B/p-RBCK1 cells were treated with 2-DG at different concentrations (0, 4, or 8 mM) for 24 h. The results

|		Intrahepatic metastasis	Lung metastasis
Hep3B-vector		3/8	2/8
Hep3B-p-RBCK1		6/8	5/8
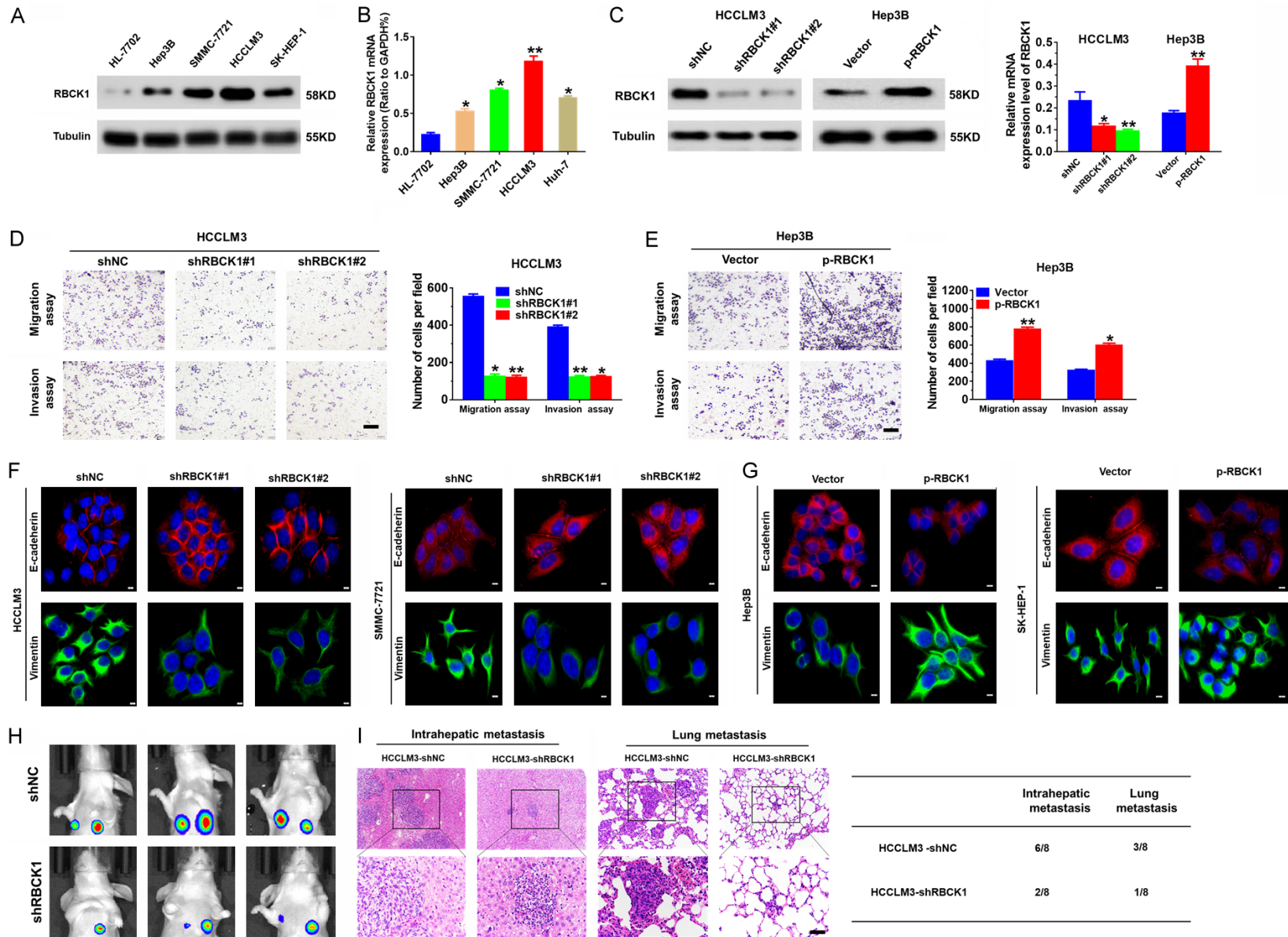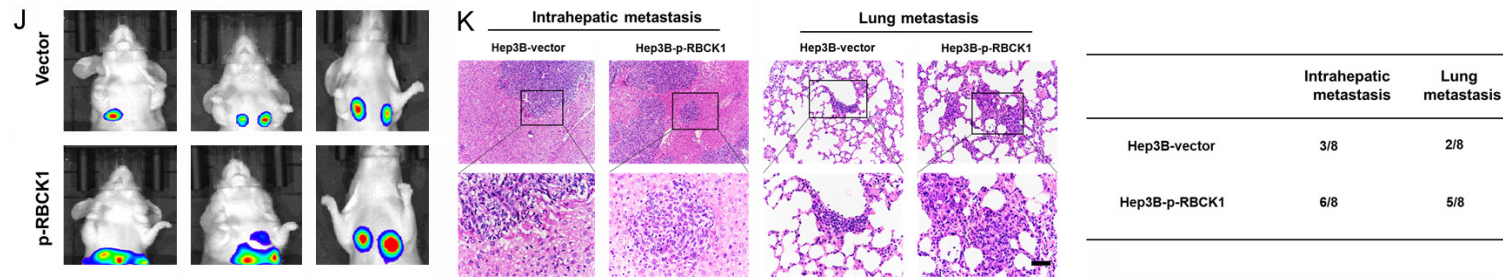
Figure 2. RBCK1 promotes the migration and invasion of HCC cells *in vitro* and accelerates the metastasis of HCC cells *in vivo*. A and B. Protein and mRNA levels of RBCK1 in HCC cell lines and normal human hepatocytes (HL-7702). C. Western blot and qRT-PCR analyses were used to detect the expression levels of RBCK1 in HCCLM3 and Hep3B cells stably transfected with the RBCK1-silenced or -overexpressing plasmid. *$P<0.05$, **$P<0.01$. D. Transwell migration and Transwell invasion assays of HCCLM3 cells transfected with RBCK1 knockdown vector. *$P<0.05$, **$P<0.01$. E. Transwell migration and Transwell invasion assays of Hep3B cells transfected with RBCK1 overexpression plasmid. F and G. Confocal microscopy analysis of E-cadherin and vimentin in RBCK1 knockdown or overexpression HCC cells. The red and green signals represent staining of the corresponding protein, and the blue signal represents the nuclear DNA staining with DAPI. H and J. Fluorescence of metastases generated in a metastasis model of orthotopic liver transplantation with stably transfected HCC cells or control cells was monitored, n=8. I and K. H&E staining of paraffin-embedded sections of intrahepatic and lung metastatic nodules. K. Statistical analysis of intrahepatic and lung metastatic nodules (n=8/group).
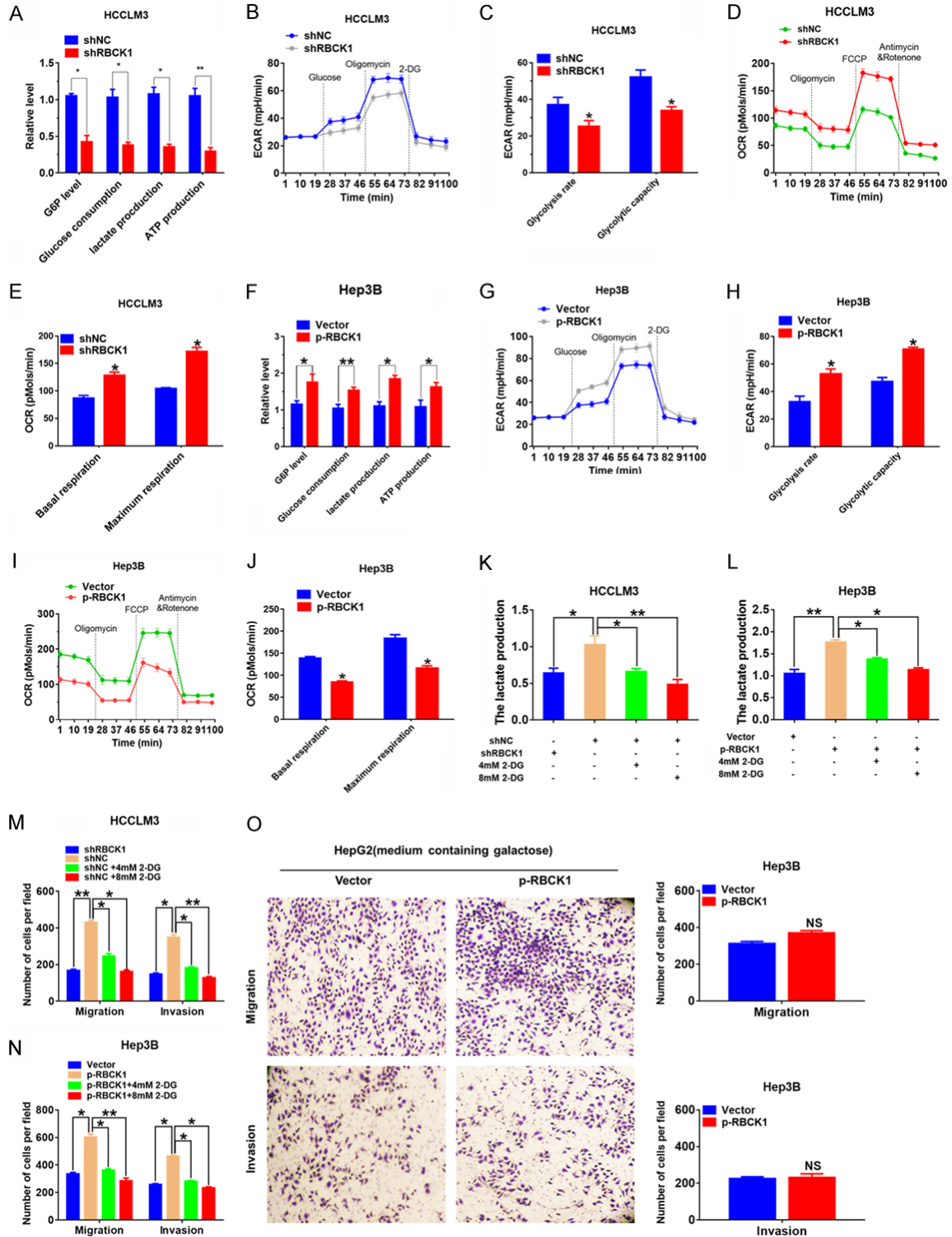
Figure 3. RBCK1 promotes the migration and invasion of HCC cells by modulating the Warburg effect. (A) Cellular G6P levels, glucose consumption, lactate production, and ATP levels in HCCLM3/shRBCK1 cells. Three independent experiments were performed. $*P<0.05$, $**P<0.01$. (B and C) ECAR data showing the glycolytic rate and capacity in RBCK1-silenced HCC cells. Glucose (10 mM), the oxidative phosphorylation inhibitor oligomycin (1.0 μM), and the glycolytic inhibitor 2-deoxyglucose (2-DG, 50 mM) were sequentially injected into each well at the indicated time points. All measurements were normalized to the cell number calculated using a crystal violet assay at the end of the experiment. $*P<0.05$. (D and E) OCR results showing basal respiration and maximum respiration in RBCK1-

silenced HCC cells. Oligomycin (1.0 µM), the mitochondrial uncoupler carbonyl cyanide p-trifluoromethoxy phenylhydrazone (FCCP, 1.0 µM), and the mitochondrial complex I inhibitor rotenone plus the mitochondrial complex III inhibitor antimycin A (Rote/AA, 0.5 µM) were sequentially injected. All measurements were normalized to the cell number calculated using a crystal violet assay at the end of the experiment. *$P<0.05$, **$P<0.01$. (F) Cellular G6P levels, glucose consumption, lactate production, and ATP levels in Hep3B/p-RBCK1 cells. (G and H) ECAR data showing the glycolytic rate and capacity in RBCK1-overexpressing HCC cells. *$P<0.05$, **$P<0.01$. (I and J) OCR results showing basal respiration and maximum respiration in RBCK1-overexpressing HCC cells. *$P<0.05$, **$P<0.01$. (K and L) Lactate production in HCCLM3/shRBCK1 (K) or Hep3B/p-RBCK1 cells (L) in the presence of 2-DG. *$P<0.05$, **$P<0.01$. (M and N) Effects of 2-DG on the migration and invasion of HCCLM3/shRBCK1 (M) or Hep3B/p-RBCK1 cells (N). *$P<0.05$, **$P<0.01$. (O) Culturing Hep3B cells in medium containing galactose but no glucose nullified the effect of RBCK1 overexpression on cell migration and invasion.

showed that in HCCLM3/shRBCK1 and Hep-3B/p-RBCK1 cells, 2-DG significantly inhibited glycolysis in a dose-dependent manner (**Figure 3K** and **3L**). The migratory and invasive abilities of HCCLM3/shRBCK1 and Hep3B/p-RBCK1 cells were also decreased in a dose-dependent manner (**Figure 3M** and **3N**). To demonstrate that glycolysis modulates HCC migration and invasion, cells were cultured in medium containing galactose instead of glucose, reducing glycolytic flux and forcing the cells to rely on oxidative phosphorylation. We observed that this reduced glycolytic flux greatly abrogated the increased migratory and invasive ability of Hep3B cells induced by RBCK1 overexpression (**Figure 3O**). These findings indicate that RBCK1 suppresses oxidative phosphorylation while promoting aerobic glycolysis (Warburg effect) in HCC cells but promotes migration and invasion by enhancing the Warburg effect in HCC cell lines *in vitro*.

RBCK1 promotes the Warburg effect via GLUT1 in HCC cells

Previous studies have demonstrated that GLUT1 plays an important role in glycolysis [19]. Thus, we speculated that RBCK1 promotes aerobic glycolysis in HCC cells via regulating GLUT1. To prove this hypothesis, we explored whether RBCK1 regulates GLUT1 expression by initially observing the expression of GLUT1 in RBCK1-knockdown and RBCK1-overexpressing HCC cells. Western blotting results revealed that RBCK1 knockdown significantly decreased GLUT1 expression in HCCLM3 cells (**Figure 4A**). Conversely, RBCK1 overexpression markedly increased GLUT1 expression in Hep3B cells (**Figure 4B**). Furthermore, upregulation of GLUT1 attenuated the loss of GLUT1 expression in HCCLM3/shRBCK1 cells (**Figure 4C**). Moreover, rescue experiments indicated that restoration of GLUT1 expression abolished the reduced metastatic ability of HCC cells induced by RBCK1 silencing (**Figure 4D** and **4E**). Importantly, the *in vivo* tumour metastasis assay revealed that overexpression of GLUT1 rescued the decreased incidence of intrahepatic and lung metastasis in HCCLM3/shRBCK1 cells (**Figure 4F**). Moreover, investigations into whether RBCK1 increases glycolysis via GLUT1 expression revealed that upregulation of GLUT1 expression rescued the RBCK1-mediated reduction in cellular G6P, glucose consumption, lactate production, and ATP levels in HCC cells (**Figure 4G**). Meanwhile, RBCK1 knockdown decreased ECAR and OCR in HCC cells, whereas simultaneous overexpression of GLUT1 attenuated the decrease in glycolytic rate and capacity (**Figure 4H-K**).

Next, we assessed the effect of decreased GLUT1 expression on RBCK1 and GLUT1 protein levels, as well as on cell migration and invasion abilities, in RBCK1-overexpressing Hep3B cells. Western blotting analyses showed that RBCK1 overexpression significantly increased GLUT1 expression, whereas knockdown of GLUT1 expression dramatically inhibited the RBCK1-induced increase in GLUT1 expression in Hep3B cells (**Figure 4L**). Moreover, GLUT1 downregulation significantly reduced RBCK1-enhanced cell migration and invasion (**Figure 4M** and **4N**). Furthermore, *in vivo* metastatic assay results revealed that GLUT1 downregulation decreased the incidence of intrahepatic and lung metastasis in the Hep3B-RBCK1 group (**Figure 4O**). Moreover, investigations into whether RBCK1 increased glycolysis via GLUT1 expression revealed that knockdown of GLUT1 expression rescued the RBCK1-mediated increase in cellular G6P, glucose consumption, lactate production, and ATP levels in HCC cells (**Figure 4P**). Meanwhile, RBCK1 overexpression increased ECAR and OCR in HCC cells, whereas simultaneous knockdown of GLUT1 attenuated the increase in glycolytic rate and capacity (**Figure 4Q-T**). Collectively, these find-
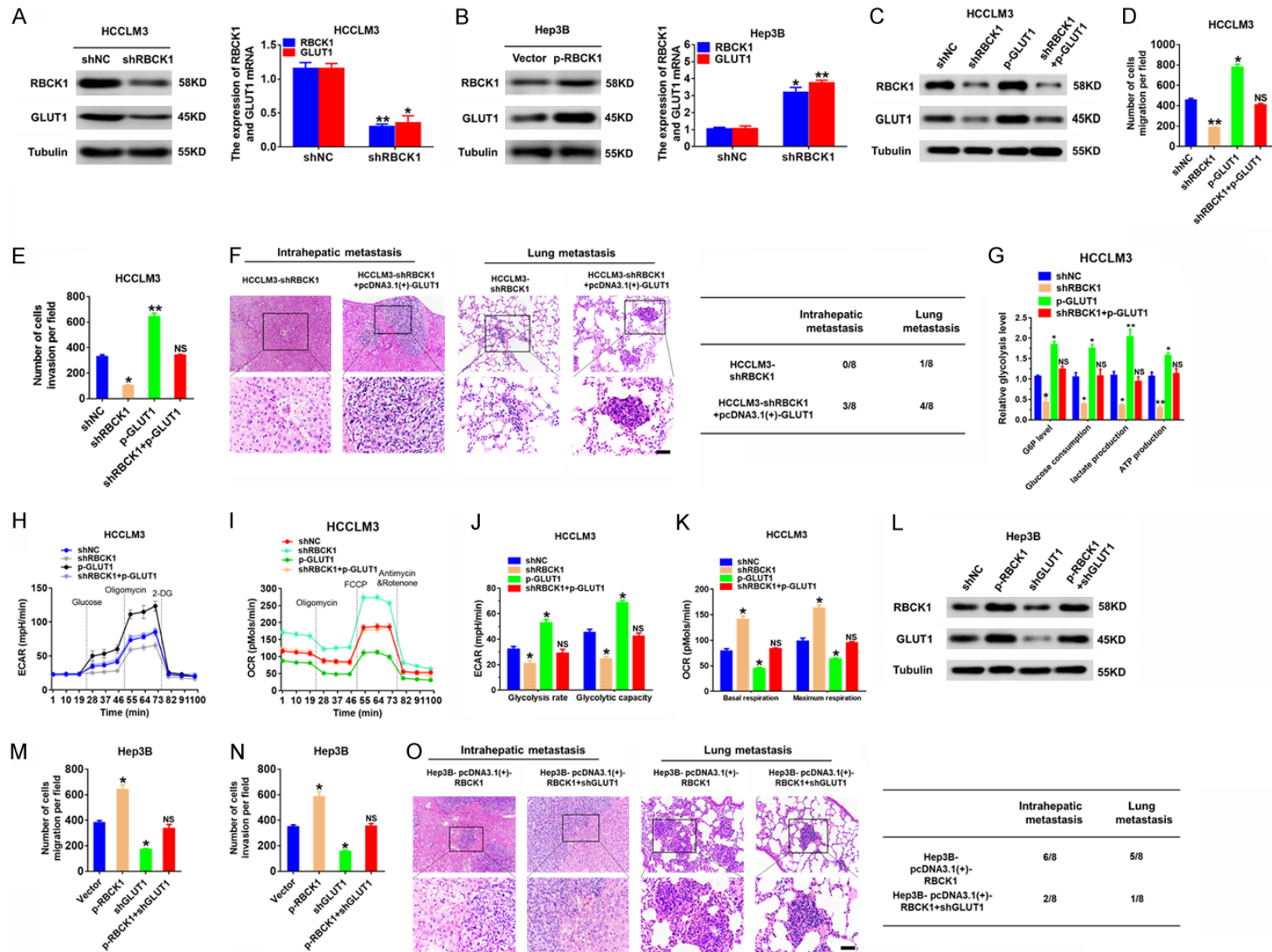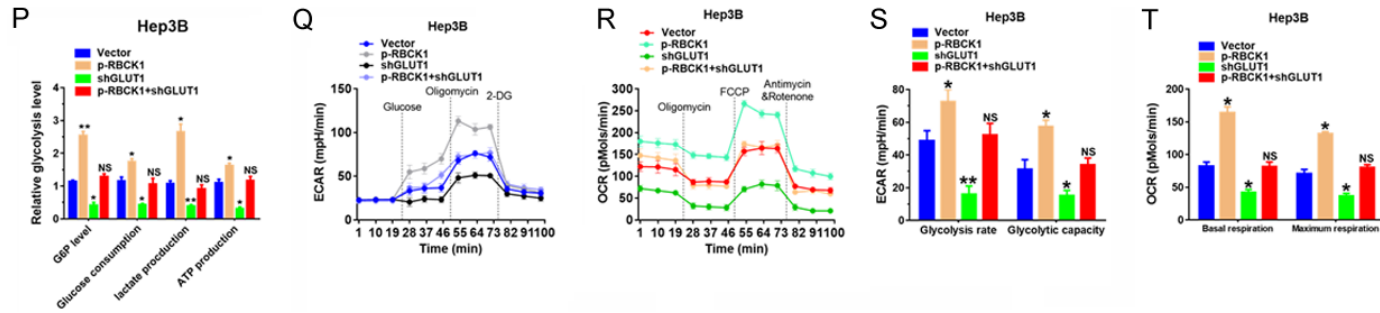
Figure 4. The effects of RBCK1 in HCC cells partially depends on modulating GLUT1 expression. (A) Western blotting and qRT-PCR analyses of GLUT1 expression levels in HCCLM3/shRBCK1 cells. *$P<0.05$, **$P<0.01$. (B) Western blotting and qRT-PCR analyses of GLUT1 expression levels in Hep3B/p-RBCK1 cells. *$P<0.05$, **$P<0.01$. (C) Western blotting was used to detect the expression of RBCK1 and GLUT1 in the different groups. Tubulin was used as a loading control. (D and E) Quantification of Transwell assays in the different groups. *$P<0.05$, **$P<0.01$. (F) Representative images (right) and quantification (left) of intrahepatic and lung metastases in the different groups of nude mice (n=8). (G) Cellular G6P levels, glucose consumption, lactate production, and ATP levels in the indicated groups. (H-K) ECAR (H and J) and OCR (I and K) were measured in the indicated groups. *$P<0.05$. (L) Western blotting was used to detect the expression of RBCK1 and GLUT1 in the indicated groups. Tubulin was used as a loading control. (M and N) Quantification of Transwell assays in the indicated groups. *$P<0.05$. (O) Representative pictures (right) and quantification (left) of intrahepatic and lung metastases in the different groups of nude mice (n=8). (P) Cellular G6P levels, glucose consumption, lactate production, and ATP levels in the indicated groups. (Q-T) ECAR (Q and S) and OCR (R and T) were measured in the indicated groups. *$P<0.05$.
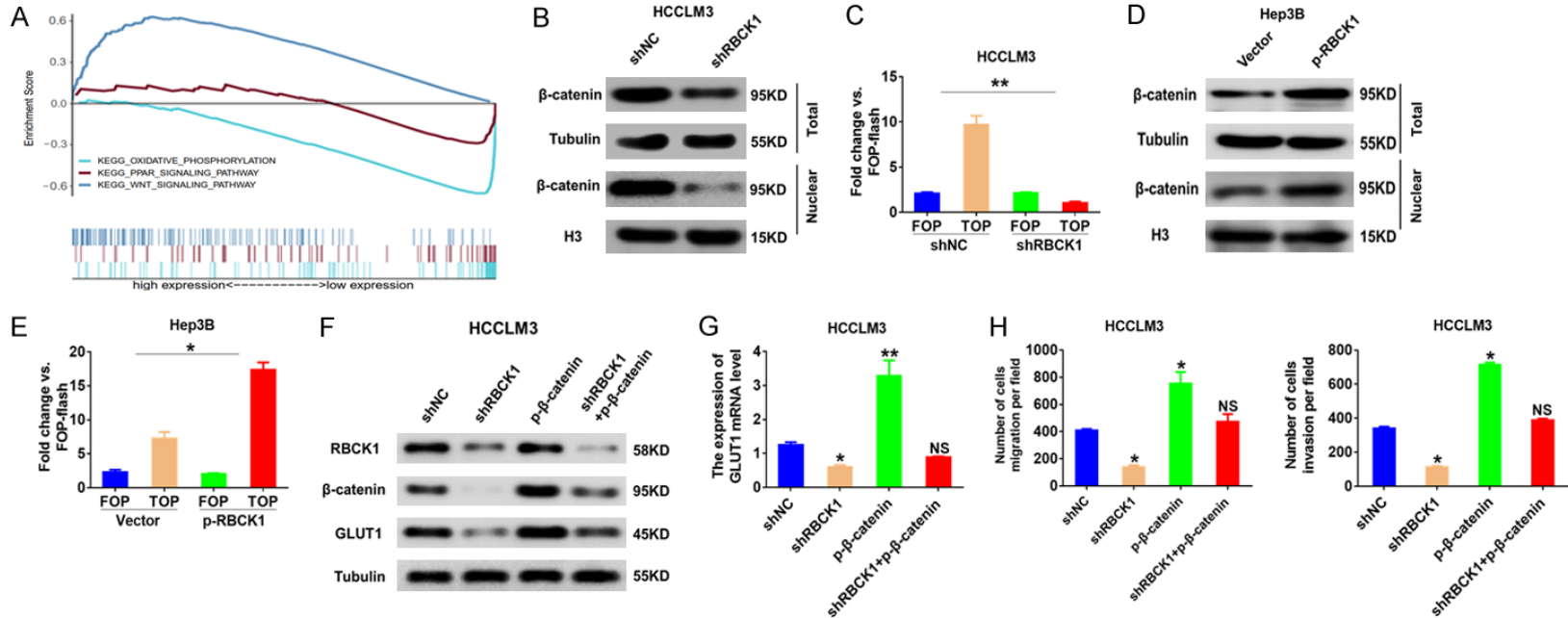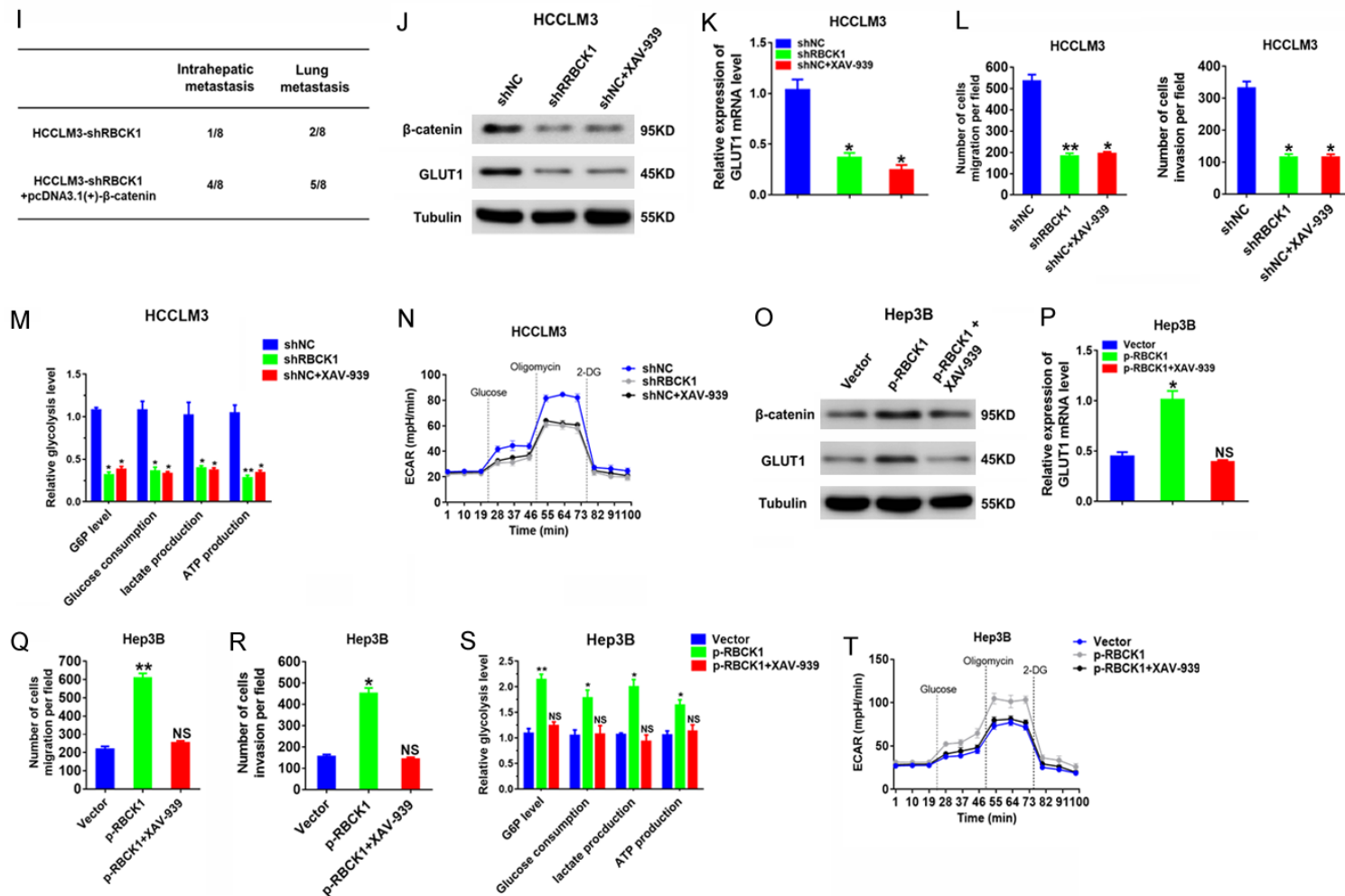
Figure 5. RBCK1 promotes a GLUT1-mediated Warburg effect via the WNT/β-catenin signalling pathway. (A) Gene set enrichment analysis (GSEA) indicated a significant change in WNT/β-catenin, oxidative phosphorylation and PPAR signalling induced by RBCK1. (B and D) The total and nuclear protein levels of β-catenin were assessed by Western blotting in RBCK1-silenced HCCLM3 cells (B) or RBCK1-overexpressing Hep3B cells (D). Tubulin and histone 3 were used as loading controls. (C and E) The relative luciferase activity levels in cells transfected with TOP-flash and FOP-flash vectors in RBCK1-silenced HCCLM3 cells (C) or RBCK1-overexpressing Hep3B cells (E) are shown. *P<0.05, **P<0.01. (F and G) Western blotting and qRT-PCR analyses of RBCK1, β-catenin and GLUT1 expression levels in the indicated groups. Tubulin was a loading control. *P<0.05, **P<0.01. (H) Quantification of Transwell assays in the indicated groups. *P<0.05, **P<0.01. (I) Quantification of intrahepatic and lung metastases in the different groups of nude mice (n=8). (J and K) Western blotting and qRT-PCR showing expression levels of RBCK1, β-catenin and GLUT1 in HCCLM3 cells transfected with shRBCK1 or treated with XAV-939. Tubulin was used as a loading control. *P<0.05. (L) Quantification of Transwell

assays in HCCLM3 cells transfected with shRBCK1 or treated with XAV-939. $^*P<0.05$, $^{**}P<0.01$. (M) Cellular G6P levels, glucose consumption, lactate production, and ATP levels in HCCLM3 cells transfected with shRBCK1 or treated with XAV-939. $^*P<0.05$, $^{**}P<0.01$. (N) ECAR was measured in HCCLM3 cells transfected with shRBCK1 or XAV-939. (O and P) Western blotting and qRT-PCR showing expression levels of RBCK1, β-catenin and GLUT1 in RBCK1-overexpressing Hep3B cells transfected with XAV-939. Tubulin was used as a loading control. $^*P<0.05$. (Q and R) Quantification of Transwell assays in RBCK1-overexpressing Hep3B cells treated with XAV-939. $^*P<0.05$, $^{**}P<0.01$. (S) Cellular G6P levels, glucose consumption, lactate production, and ATP levels in RBCK1-overexpressing Hep3B cells treated with XAV-939. $^*P<0.05$, $^{**}P<0.01$. (T) ECAR was measured in RBCK1-overexpressing Hep3B cells treated with XAV-939.

ings indicated that GLUT1 is a functional downstream target of RBCK1 in the regulation of aerobic glycolysis and that it is critical in RBCK1-mediated tumour progression.

RBCK1-induced activation of GLUT1 is mediated by WNT/β-catenin signaling

To further clarify the mechanism by which RBCK1 regulates GLUT1 in HCC, the Gene set enrichment analysis (GSEA) was performed to determine the effects of transcriptomic changes on biological functions and pathways. The WNT signalling pathway was significantly positively correlated with RBCK1 in HCCLM3 cells (**Figure 5A**). Because GLUT1 is a target gene of WNT/β-catenin, we speculated that RBCK1 regulates GLUT1 via the WNT/β-catenin signalling pathway. To test this hypothesis, we measured changes in β-catenin expression in RBCK1-knockdown HCCLM3 cells. Western blotting analyses revealed that total and nuclear β-catenin protein expression levels were decreased in response to decreasing RBCK1 expression in HCCLM3 cells (**Figure 5B**). The TOP-Flash reporter luciferase assay demonstrated that RBCK1 knockdown decreased the transcriptional activity of TCF4 in HCCLM3 cells compared to the shNC control in HCCLM3 cells (**Figure 5C**). In contrast, RBCK1 overexpression generated the opposite effects in Hep3B cells (**Figure 5D** and **5E**). We further determined that β-catenin upregulation rescued the decrease in GLUT1 expression, cell migration, and cell invasion induced by RBCK1 knockdown (**Figure 5F-I**).

To verify that RBCK1 regulates GLUT1 expression through the WNT/β-catenin signalling pathway, we measured levels of GLUT1 and β-catenin in the presence of the WNT/β-catenin pathway inhibitor XAV-939. Consistently, XAV-939 inhibited mRNA and protein levels of GLUT1 in HCCLM3 cells (**Figure 5J** and **5K**). Transwell assays demonstrated that XAV-939 markedly decreased cell migration and inva-

sion (**Figure 5L**). XAV-939 led to a decrease in cellular G6P, glucose consumption, lactate production, and ATP levels in HCC cells (**Figure 5M**). Meanwhile, XAV-939 inhibited ECAR in HCC cells (**Figure 5N**). Moreover, rescue experiments indicated that XAV-939 treatment attenuated the enhanced metastatic ability and Warburg effect of HCC cells induced by RBCK1 overexpression (**Figure 5O-T**). Consistently, β-catenin silencing abolished the increased metastatic ability and Warburg effect of HCC cells induced by RBCK1 overexpression (Figure S3). Taken together, RBCK1 promotes metastasis of HCC cells via the GLUT1-mediated Warburg effect through activation of WNT/β-catenin signalling.

RBCK1 destroys the PPARγ/PGC1α complex to activate the WNT/β-catenin pathway and Warburg effect in HCC cells

To clarify the mechanism through which RBCK1 regulates the WNT/β-catenin signalling pathway in HCC cells, we first determined whether there was a direct interaction between the RBCK1 and β-catenin proteins. Co-IP indicated that no direct interaction existed between these proteins (**Figure 6A**). The PPARγ/PGC1α complex inhibits the canonical WNT/β-catenin pathway and contributes to glucose homeostasis. Therefore, we speculated that RBCK1 regulated WNT/β-catenin via destruction of the PPARγ/PGC1α complex. To test this hypothesis, we first determined whether RBCK1 influenced the activation of the β-catenin/GLUT1 pathway via destruction of the PPARγ/PGC1α complex. Changes in β-catenin, GLUT1, PGC1α, and PPARγ expression, as well as in the PPARγ/PGC1α complex, were measured in RBCK1-knockdown HCC cells. The results demonstrated that RBCK1 knockdown in HCCLM3 cells significantly increased levels of PPARγ expression and the PPARγ/PGC1α complex and decreased β-catenin and GLUT1 expression but produced no change in PGC1α protein levels (**Figure 6B** and **6C**). In contrast, RBCK1 overex-
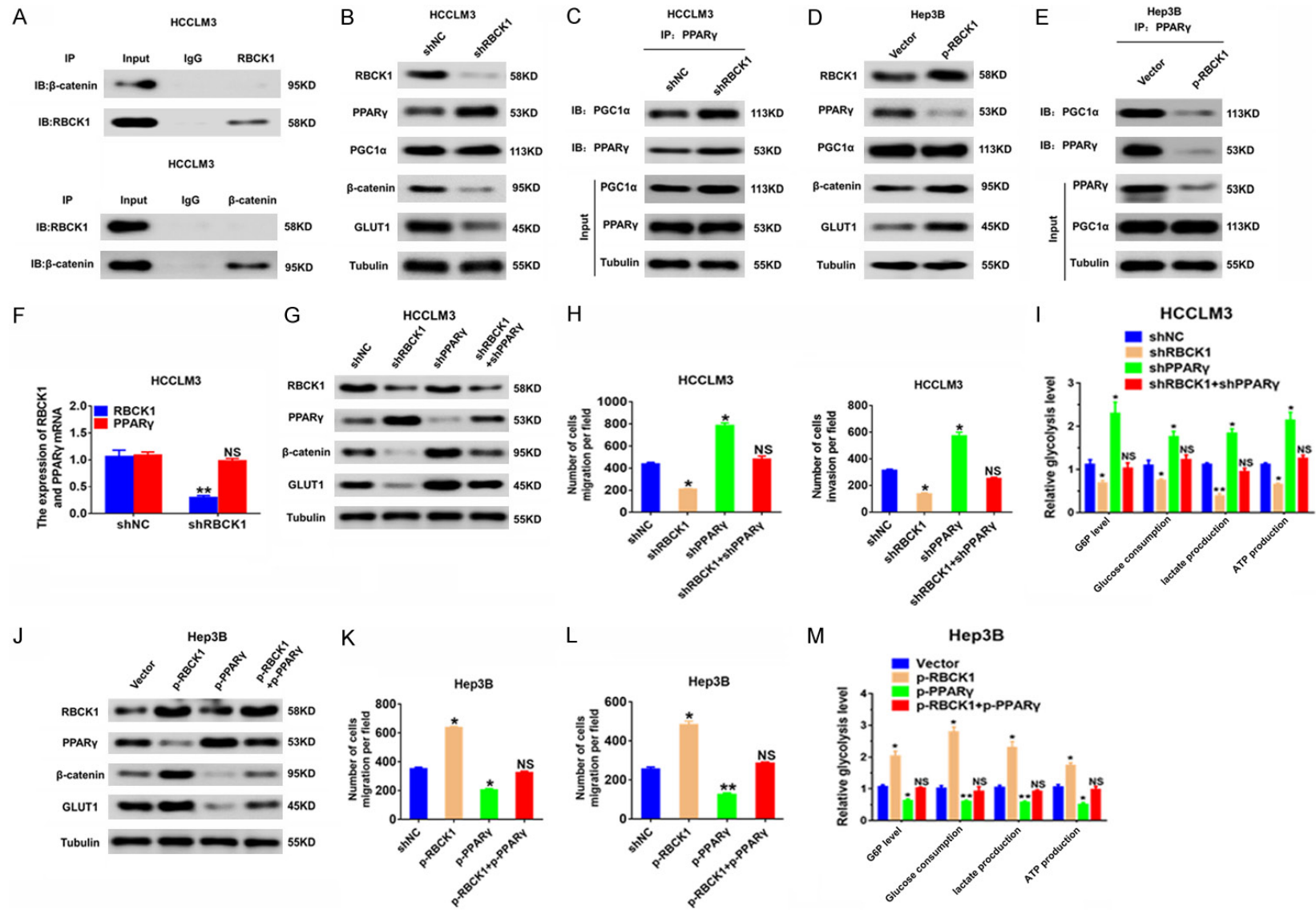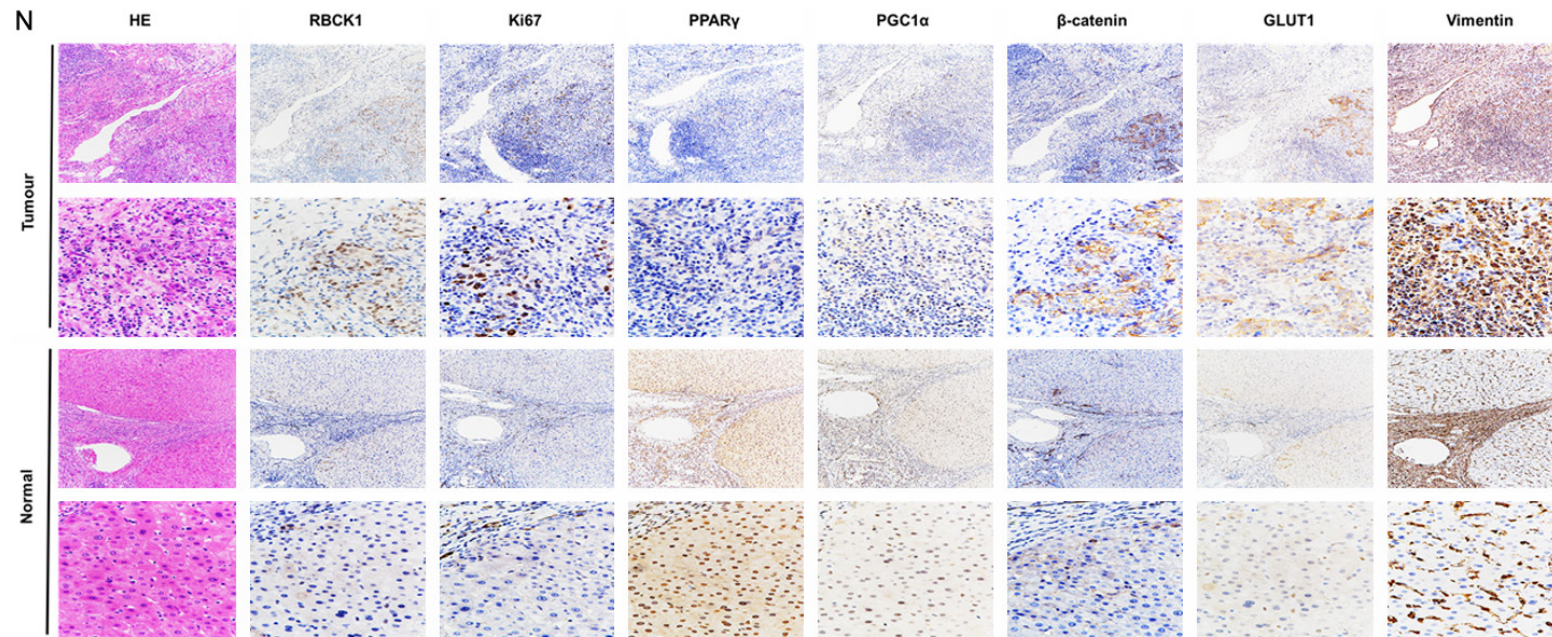
Figure 6. RBCK1 activates the WNT/β-catenin pathway and the Warburg effect in HCC cells by destroying the PPARγ/PGC1α complex. A. The Co-IP assay showed no interaction between RBCK1 and β-catenin. B. Western blotting showing expression levels of RBCK1, PPARγ, PGC1α, β-catenin and GLUT1 in RBCK1-silenced HCCLM3 cells. Tubulin was used as a loading control. C. Co-IP combined with Western blotting assay showing the expression levels of PPARγ and PGC1α in RBCK1-silenced HCCLM3 cells. Tubulin was used as a loading control. D. Western blotting showing expression levels of RBCK1, PPARγ, PGC1α, β-catenin and GLUT1 in RBCK1-overexpressing Hep3B cells. Tubulin was used as a loading control. E. Co-IP combined with Western blotting assay showing expression levels of PPARγ and PGC1α in RBCK1-overexpressing Hep3B cells. Tubulin was used as a loading control. F. qRT-PCR showing expression levels of RBCK1 and PPARγ in RBCK1-silenced HCCLM3 cells. G. Western blotting showing expression levels of RBCK1, PPARγ, β-catenin and GLUT1 in RBCK1-silenced HCCLM3 cells transfected with shPPARγ. Tubulin was used as a loading control. H. Quantification of Transwell assays in RBCK1-silenced HCCLM3 cells transfected with shPPARγ. $^{*}P<0.05$. I. Cellular G6P levels, glucose consumption, lactate production, and ATP levels in RBCK1-silenced HCCLM3 cells transfected with shPPARγ. $^{*}P<0.05$, $^{**}P<0.01$. J. Western blotting showing the expression levels of RBCK1, PPARγ, β-catenin and GLUT1 in RBCK1-overexpressing Hep3B cells transfected with p-PPARγ. Tubulin was a loading control. K and L. Quantification of Transwell assays in RBCK1-overexpressing Hep3B cells transfected with p-PPARγ. $^{*}P<0.05$. M. Cellular G6P levels, glucose consumption, lactate production, and ATP levels in RBCK1-silenced HCCLM3 cells transfected with shPPARγ. $^{*}P<0.05$, $^{**}P<0.01$. N. Immunohistochemistry was employed to identify the protein expression of RBCK1, Ki67, PPARγ, PGC1α, β-catenin, GLUT1 and vimentin in HCC tissues and their adjacent noncarcinoma normal tissues. Scale bar, 50 μm.
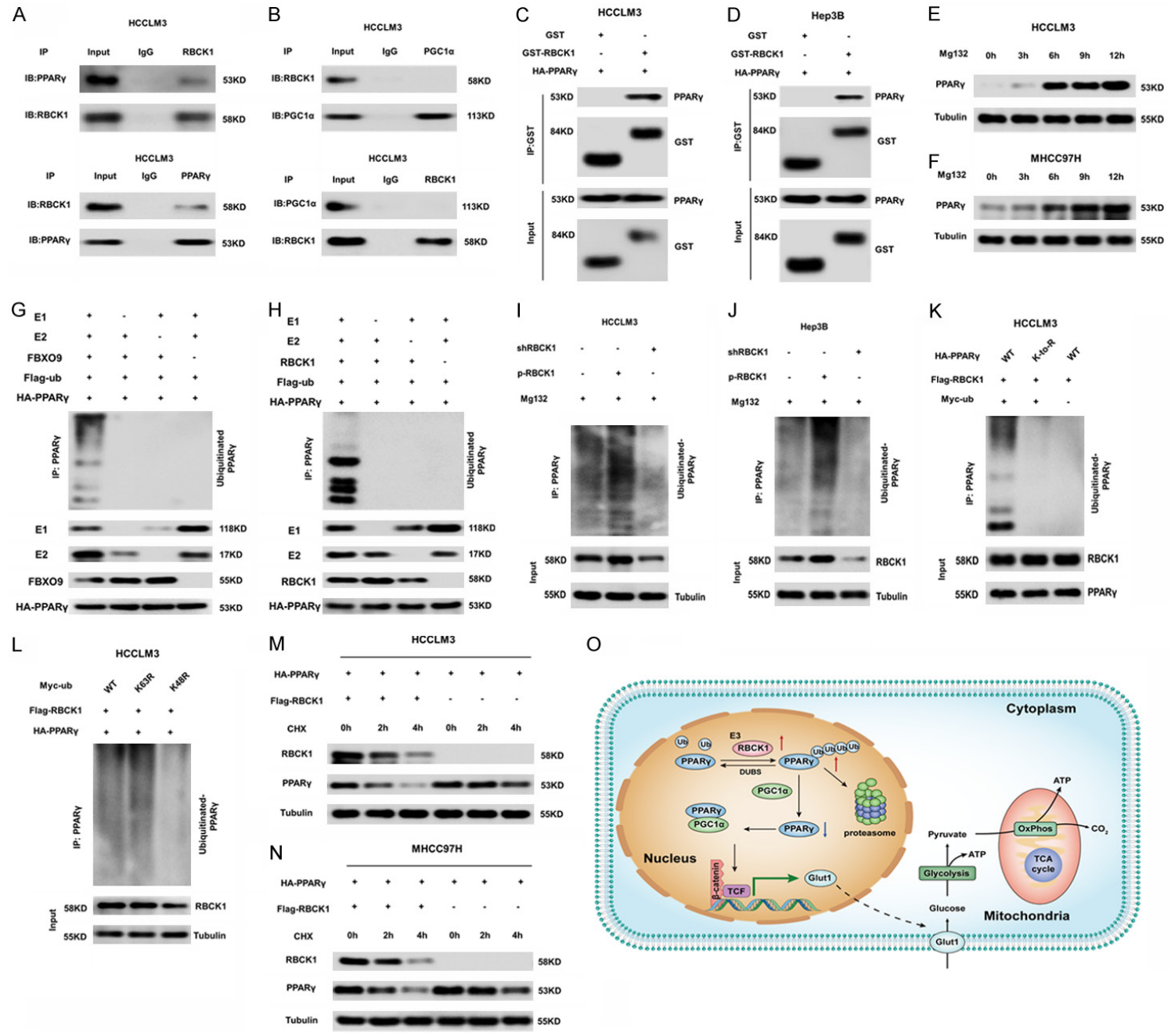
Figure 7. RBCK1 interacts and destabilizes PPARγ by promoting PPARγ ubiquitination and degradation in HCC cells. A. Co-IP showing direct binding of endogenous RBCK1 and PPARγ in HCCLM3 cells. B. Co-IP showing that endogenous RBCK1 and PPARγ were not directly bound. C and D. GST pulldown assay showing that RBCK1 and PPARγ directly bind in HEK293 cells. E and F. HCC cells were treated with MG132 (Z-Leu-Leu-Leu-CHO, 15 μmol/L) for the indicated times, and the levels of PPARγ were determined. G and H. The ubiquitination level of HA-PPARγ was detected in the presence of E1, E2 (UBCH5c), FBXO9, RBCK1 and Ub in HEK293 cells. I and J. Knockdown or overexpression of RBCK1 altered the ubiquitination of PPARγ. The cells in each group were treated with the proteasomal inhibitor MG132. Cell lysates were prepared and subjected to immunoprecipitation using an anti-PPARγ antibody. Levels of ubiquitin-attached PPARγ were detected by Western blotting with an anti-Ub antibody. K. Ubiquitination of wild type PPARγ or the K-to-R mutant (mutations in all Lys sites of the PPARγ gene) in HEK293 cells. L. Measurement of the PPARγ ubiquitination type in HEK293 cells. M and N. HCC cells were transfected with a plasmid encoding HA-PPARγ either with or without the Flag-RBCK1 plasmid. Then, the cells were subjected to cycloheximide (CHX) (20 μmol/L) exposure at the indicated times, and the degradation of PPARγ was detected using an anti-HA antibody. O. Proposed model by which the E3 ubiquitin ligase RBCK1 promotes the GLUT1-mediated Warburg effect by destroying the PPARγ/PGC1α complex.

pression in Hep3B cells significantly decreased the levels of PPARγ protein expression and the PPARγ/PGC1α complex and increased β-catenin and GLUT1 expression while also producing no change in PGC1α protein levels (**Figure 6D** and **6E**). In addition, the PPARγ mRNA levels in HCC cells remained unaffected by changes in RBCK1 expression (**Figures 6F** and **S4**). The PPARγ/PGC1α complex is therefore involved in RBCK1-mediated regulation of the β-catenin/GLUT1 pathway.

To verify that RBCK1 regulates the β-catenin/GLUT1 pathway through destruction of the PPARγ/PGC1α complex, PPARγ was knocked down in RBCK1-downregulated HCC cells, and PPARγ downregulation inhibited the decrease in β-catenin and GLUT1 expression, cell migration, and aerobic glycolysis observed in RBCK1-knockdown HCCLM3 cells (**Figure 6G-I**). In contrast, PPARγ upregulation inhibited the increase in β-catenin and GLUT1 expression, cell migration, and aerobic glycolysis observed in RBCK1-upregulated HepG2 cells (**Figure 6J-M**). Importantly, IHC staining (**Figure 6N**) revealed that compared to adjacent nontumorbearing tissues, the RBCK1, Ki67, β-catenin, GLUT1 and vimentin proteins were upregulated, whereas PPARγ and PGC1α were downregulated in HCC tissues. These results indicated that the RBCK1-mediated regulation of β-catenin/GLUT1 pathway-induced HCC cell migration and aerobic glycolysis is therefore dependent on destruction of the PPARγ/PGC1α complex.

RBCK1 disrupts the PPARγ/PGC1α complex by promoting the ubiquitination and degradation of PPARγ

RBCK1 interacts with different substrates to exert its effects. We next examined whether

RBCK1, PPARγ, and PGC1α directly interacted in HCC cells. Co-IP analysis detected endogenous RBCK1 and PPARγ in the immunoprecipitate, indicating an interaction between RBCK1 and PPARγ but no direct interaction between RBCK1 and PGC1α (**Figure 7A** and **7B**). Moreover, a GST pulldown assay indicated that RBCK1 binds to PPARγ in an *in vitro* system (**Figure 7C** and **7D**). These findings confirmed that RBCK1 directly binds to PPARγ in HCC cells and that RBCK1 disrupts the PPARγ/PGC1α complex by regulating PPARγ expression.

We next assessed the mechanisms by which RBCK1 regulates PGC1α. Consistent with findings from a previous study showing PPARγ degradation via the UPS, treatment with the proteasome inhibitor MG132 led to significant accumulation of endogenous PPARγ protein in HCC cells (**Figure 7E** and **7F**). Moreover, the data indicate efficient ubiquitination of His-PPARγ was in the presence of E1, E2 (UBCH5c), FBXO9 (an E3 ubiquitin ligase for PPARγ), RBCK1 and Ub (**Figure 7G** and **7H**). PPARγ is therefore also degraded by the UPS in HCC cells. Next, we determined whether RBCK1 could directly mediate PPARγ ubiquitination. Interestingly, PPARγ polyubiquitination was substantially increased by ectopic RBCK1 expression but decreased by RBCK1 knockdown (**Figure 7I** and **7J**). The data also showed that mutations in all the Lys sites of PPARγ abolished its polyubiquitination (**Figure 7K**). As expected, mutation of the Lys48 site on ubiquitin (Ub) almost entirely abolished RBCK1-mediated PPARγ ubiquitination, whereas the K63R mutation produced no effect (**Figure 7L**). Consistent with the ubiquitination results, a degradation dynamics assay confirmed that the half-life of exogenously expressed PPARγ was significantly decreased in RBCK1-over-

expressing HCC cells compared to that in control cells (**Figure 7M** and **7N**). These data indicate that RBCK1 mediates Lys48-linked polyubiquitination of PPARγ, which leads to PPARγ degradation by the proteasome. Collectively, these results indicate that RBCK1 destroys the PPARγ/PGC1α complex by promoting PPARγ ubiquitination and degradation (**Figure 7O**).

Discussion

HCC is one of the most common malignant tumours in the world and the second leading cause of cancer-related deaths [24]. Despite major improvements in diagnosis and treatment methods, metastasis remains the primary cause of treatment failure and death [25]. Although modern multidisciplinary nursing strategies have been applied to treat tumour metastasis, the overall five-year survival rate remains only 25%-39%, with a recurrence rate of approximately 80% in patients with advanced liver cancer [26]. Metastasis of a malignant tumour is often the primary reason for treatment failure in patients with liver cancer [27]. Moreover, the molecular mechanism of HCC metastasis is still unclear. In the present study, we determined that high RBCK1 expression predicts poor HCC prognosis and that RBCK1 accelerates the metastasis of HCC through an enhanced GLUT1-mediated Warburg effect resulting in destruction of the PPARγ/PGC1α complex.

As a key regulator of the unfolded protein response in the development of cancer, RBCK1 was initially identified during the screening of progesterone regulatory genes in human breast cancer cells [28]. RBCK1 overexpression promotes the progression of lung adenocarcinoma, CRC and renal cell carcinoma [29]. Several studies have highlighted the involvement of RBCK1 in many aspects of cancer biology, and many of its molecular functions are consistent with its role in cancer. However, there is no information regarding the specific role or molecular mechanism of RBCK1 in HCC. Here, we found that RBCK1 expression is upregulated and is associated with poor prognosis in HCC patients. Additionally, RBCK1 expression was correlated with tumour size and vascular invasion. Ectopic expression of RBCK1 markedly promoted HCC migration and invasion both *in vitro* and *in vivo*. Moreover, our results revealed

that RBCK1 promotes aerobic glycolysis and inhibits mitochondrial respiration in HCC cells. These findings are important not only to better understand the biological functions of RBCK1 in cancer but also for assessing the potential of RBCK1 as a therapeutic target.

Aerobic glycolysis, also known as the Warburg effect, is the most characteristic metabolic phenotype of cancer cells, including HCC [30]. The Warburg effect is due to oncogene activation and overexpression of glucose transporters or enzymes from the glycolysis pathway. The destruction of tumour cell metabolism can inhibit metastasis, indicating that aerobic glycolysis is at the core of tumour growth and survival [30, 31]. Therefore, it is very important to obtain an in-depth understanding of the relationship between cell metabolism and tumour metastasis to develop new treatment methods against liver cancer. Here, we describe a novel mechanism wherein RBCK1 promotes HCC invasion and metastasis by upregulating a GLUT1-mediated Warburg effect. First, our data indicated that high RBCK1 and GLUT1 levels exist in HCC tissues compared to adjacent nontumor-bearing tissues. We also found that RBCK1 inhibition reduces GLUT1 expression and decreases aerobic glycolysis and metastasis in HCC *in vitro* and *in vivo*. Moreover, GLUT1 upregulation rescued the decreased aerobic glycolysis and lung metastasis induced by RBCK1 knockdown, whereas GLUT1 inhibition significantly decreased RBCK1-enhanced aerobic glycolysis and metastasis. These findings suggest that GLUT1 is a functional downstream target of RBCK1 in the regulation of aerobic glycolysis and is critical for RBCK1-mediated tumour metastasis.

As a downstream target of WNT/β-catenin signalling, GLUT1 plays important roles in glycolysis and chemotherapeutic resistance in HCC [32]. Here, we determined that decreases in GLUT1 expression, cell migration, and invasion induced by RBCK1 knockdown were rescued by β-catenin upregulation. The WNT/β-catenin pathway inhibitors XAV-939 and ICG-001 notably decreased RBCK1-induced cell migration and invasion. Furthermore, RBCK1 knockdown in HCC cells significantly increased PPARγ expression and the PPARγ/PGC1α complex but decreased β-catenin and GLUT1 expression while producing no change in PGC1α protein

levels. Downregulation of PPARγ inhibited the decreases in β-catenin and GLUT1 expression, cell migration, and aerobic glycolysis observed in RBCK1-knockdown HCC cells. Our findings demonstrated for the first time that RBCK1-mediated regulation of WNT/β-catenin/GLUT1 pathway-induced HCC cell migration and aerobic glycolysis is dependent on destruction of the PPARγ/PGC1α complex.

Finally, we investigated the mechanism by which RBCK1 destroyed the PPARγ/PGC1α complex. Posttranslational modification by E3 ubiquitin ligases can modulate the functions of target proteins, their fate, and their intracellular mechanisms [17]. RBCK1 interacts with different substrates to exert its effects. Studies have reported that ubiquitin-proteasome-mediated degradation of PPARγ is the critical mechanism by which PPARγ levels are regulated in cells [33]. Similarly, our results suggest, for the first time, that RBCK1 destroys the PPARγ/PGC1α complex by promoting the ubiquitination and degradation of PPARγ. This conclusion is based on the following observations. First, RBCK1 directly binds to PPARγ in HCC cells, as indicated by Co-IP analyses. Second, efficient ubiquitination of His-PPARγ occurred in the presence of E1, E2 (UBCH5c), FBXO9 (an E3 ubiquitin ligase for PPARγ), and Ub. Next, PPARγ polyubiquitination was increased in response to RBCK1 overexpression but decreased by RBCK1 knockdown. Mutations in all the Lys sites of PPARγ abolished PPARγ polyubiquitination. Finally, mutation of the Lys48 site of ubiquitin completely abolished RBCK1-mediated PPARγ ubiquitination, whereas the K63R mutation on Ub produced no effect.

In summary, our study generated initial evidence associating high levels of RBCK1 expression with poor prognosis in HCC patients and revealed the molecular mechanism of RBCK1 during the metabolism and progression of HCC. We also demonstrated that RBCK1 promotes HCC cell metastasis by enhancing the Warburg effect via GLUT1. More importantly, RBCK1-mediated regulation of WNT/β-catenin/GLUT1 pathway-induced HCC cell migration and aerobic glycolysis is dependent on destruction of the PPARγ/PGC1α complex. Based on these findings, RBCK1 has the potential to serve as a candidate biomarker for the future diagnosis and treatment of HCC.

Disclosure of conflict of interest

None.

Address correspondence to: Tiande Liu, Department of General Surgery, The Second Affiliated Hospital of Nanchang University, Nanchang 330000, Jiangxi Province, China. Tel: +86-791-86895550; Fax: +86-791-86895863; E-mail: ndefyltd0791@163.com

References

[1] Vander Heiden MG, Cantley LC and Thompson CB. Understanding the Warburg effect: the metabolic requirements of cell proliferation. Science 2009; 324: 1029-1033.

[2] Liberti MV and Locasale JW. The Warburg effect: how does it benefit cancer cells? Trends Biochem Sci 2016; 41: 211-218.

[3] Wei J, Wu J, Xu W, Nie H, Zhou R, Wang R, Liu Y, Tang G and Wu J. Salvianolic acid B inhibits glycolysis in oral squamous cell carcinoma via targeting PI3K/AKT/HIF-1α signaling pathway. Cell Death Dis 2018; 9: 599.

[4] Xia L, Sun J, Xie S, Chi C, Zhu Y, Pan J, Dong B, Huang Y, Xia W, Sha J and Xue W. PRKAR2B-HIF-1α loop promotes aerobic glycolysis and tumour growth in prostate cancer. Cell Prolif 2020; 53: e12918.

[5] Lunt SY and Vander Heiden MG. Aerobic glycolysis: meeting the metabolic requirements of cell proliferation. Annu Rev Cell Dev Biol 2011; 27: 441-464.

[6] Deng D, Xu C, Sun P, Wu J, Yan C, Hu M and Yan N. Crystal structure of the human glucose transporter GLUT1. Nature 2014; 510: 121-125.

[7] Zambrano A, Molt M, Uribe E and Salas M. Glut 1 in cancer cells and the inhibitory action of resveratrol as a potential therapeutic strategy. Int J Mol Sci 2019; 20: 3374.

[8] Amann T and Hellerbrand C. GLUT1 as a therapeutic target in hepatocellular carcinoma. Expert Opin Ther Targets 2009; 13: 1411-1427.

[9] Wu Q, Ba-Alawi W, Deblois G, Cruickshank J, Duan S, Lima-Fernandes E, Haight J, Toneka-

boni SAM, Fortier AM, Kuasne H, McKee TD, Mahmoud H, Kushida M, Cameron S, Dogan-Artun N, Chen W, Nie Y, Zhang LX, Vellanki RN, Zhou S, Prinos P, Wouters BG, Dirks PB, Done SJ, Park M, Cescon DW, Haibe-Kains B, Lupien M and Arrowsmith CH. GLUT1 inhibition blocks growth of RB1-positive triple negative breast cancer. Nat Commun 2020; 11: 4205.

[10] Ozerlat I. Kidney cancer: targeted therapy of glucose uptake via GLUT1 kills RCC cells. Nat Rev Urol 2011; 8: 471.

[11] Chen J, Cao L, Li Z and Li Y. SIRT1 promotes GLUT1 expression and bladder cancer progression via regulation of glucose uptake. Hum Cell 2019; 32: 193-201.

[12] Sun M, Zhao S, Duan Y, Ma Y, Wang Y, Ji H and Zhang Q. GLUT1 participates in tamoxifen resistance in breast cancer cells through autophagy regulation. Naunyn Schmiedebergs Arch Pharmacol 2021; 394: 205-216.

[13] Ravid T and Hochstrasser M. Diversity of degradation signals in the ubiquitin-proteasome system. Nat Rev Mol Cell Biol 2008; 9: 679-690.

[14] Popovic D, Vucic D and Dikic I. Ubiquitination in disease pathogenesis and treatment. Nat Med 2014; 20: 1242-1253.

[15] Swatek KN and Komander D. Ubiquitin modifications. Cell Res 2016; 26: 399-422.

[16] Zheng N and Shabek N. Ubiquitin ligases: structure, function, and regulation. Annu Rev Biochem 2017; 86: 129-157.

[17] Berndsen CE and Wolberger C. New insights into ubiquitin E3 ligase mechanism. Nat Struct Mol Biol 2014; 21: 301-307.

[18] Wang P, Dai X, Jiang W, Li Y and Wei W. RBR E3 ubiquitin ligases in tumorigenesis. Semin Cancer Biol 2020; 67: 131-144.

[19] Zhang Z, Li X, Yang F, Chen C, Liu P, Ren Y, Sun P, Wang Z, You Y, Zeng YX and Li X. DHHC9-mediated GLUT1 S-palmitoylation promotes glioblastoma glycolysis and tumorigenesis. Nat Commun 2021; 12: 5872.

[20] Liu ML, Zang F and Zhang SJ. RBCK1 contributes to chemoresistance and stemness in colorectal cancer (CRC). Biomed Pharmacother 2019; 118: 109250.

[21] Yu S, Dai J, Ma M, Xu T, Kong Y, Cui C, Chi Z, Si L, Tang H, Yang L, Sheng X and Guo J. RBCK1 promotes p53 degradation via ubiquitination in renal cell carcinoma. Cell Death Dis 2019; 10: 254.

[22] Tatematsu K, Yoshimoto N, Okajima T, Tanizawa K and Kuroda S. Identification of ubiquitin ligase activity of RBCK1 and its inhibition by splice variant RBCK2 and protein kinase Cbeta. J Biol Chem 2008; 283: 11575-11585.

[23] Xiao H, Wang J, Yan W, Cui Y, Chen Z, Gao X, Wen X and Chen J. GLUT1 regulates cell glycolysis and proliferation in prostate cancer. Prostate 2018; 78: 86-94.

[24] Siegel RL, Miller KD, Fuchs HE and Jemal A. Cancer statistics, 2021. CA Cancer J Clin 2021; 71: 7-33.

[25] Yang JD, Hainaut P, Gores GJ, Amadou A, Plymoth A and Roberts LR. A global view of hepatocellular carcinoma: trends, risk, prevention and management. Nat Rev Gastroenterol Hepatol 2019; 16: 589-604.

[26] Kulik L and El-Serag HB. Epidemiology and management of hepatocellular carcinoma. Gastroenterology 2019; 156: 477-491, e471.

[27] Wang H, Lu Z and Zhao X. Tumorigenesis, diagnosis, and therapeutic potential of exosomes in liver cancer. J Hematol Oncol 2019; 12: 133.

[28] Gustafsson N, Zhao C, Gustafsson JA and Dahlman-Wright K. RBCK1 drives breast cancer cell proliferation by promoting transcription of estrogen receptor alpha and cyclin B1. Cancer Res 2010; 70: 1265-1274.

[29] Queisser MA, Dada LA, Deiss-Yehiely N, Angulo M, Zhou G, Kouri FM, Knab LM, Liu J, Stegh AH, DeCamp MM, Budinger GR, Chandel NS, Ciechanover A, Iwai K and Sznajder JI. HOIL-1L functions as the PKCζ ubiquitin ligase to promote lung tumor growth. Am J Respir Crit Care Med 2014; 190: 688-698.

[30] Gatenby RA and Gillies RJ. Why do cancers have high aerobic glycolysis? Nat Rev Cancer 2004; 4: 891-899.

[31] Lebelo MT, Joubert AM and Visagie MH. Warburg effect and its role in tumourigenesis. Arch Pharm Res 2019; 42: 833-847.

[32] Zhao Z, Wang L, Bartom E, Marshall S, Rendleman E, Ryan C, Shilati A, Savas J, Chandel N and Shilatifard A. β-catenin/Tcf7l2-dependent transcriptional regulation of GLUT1 gene expression by Zic family proteins in colon cancer. Sci Adv 2019; 5: eaax0698.

[33] Sun L and Bian K. The nuclear export and ubiquitin-proteasome-dependent degradation of PPARγ induced by angiotensin II. Int J Biol Sci 2019; 15: 1215-1224.
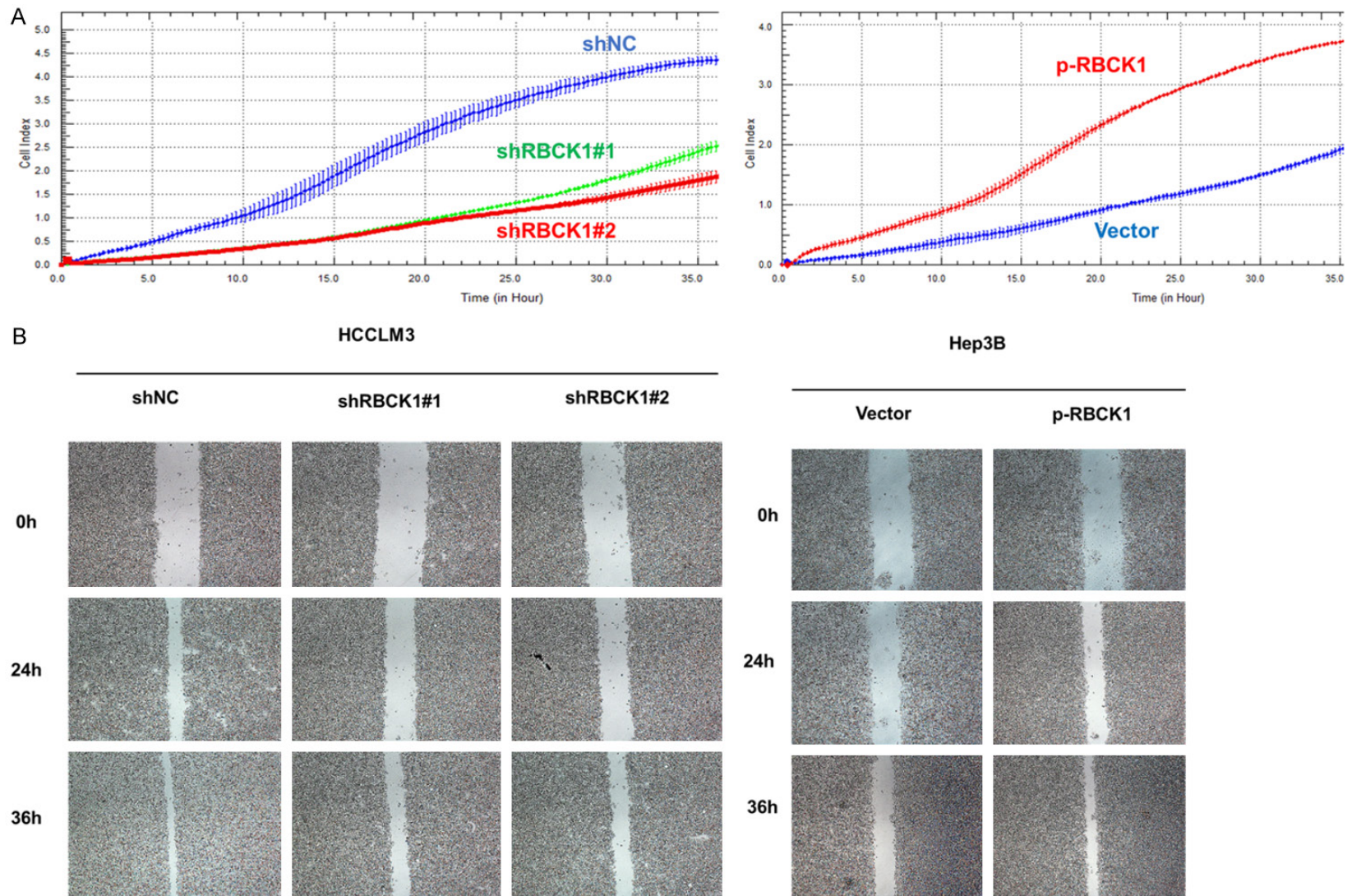
Figure S1. (A and B) Migratory properties of HCC cells with PGC1α overexpression compared to control vector group were analyzed using RTCA (A) and scratch wound healing assays (B).
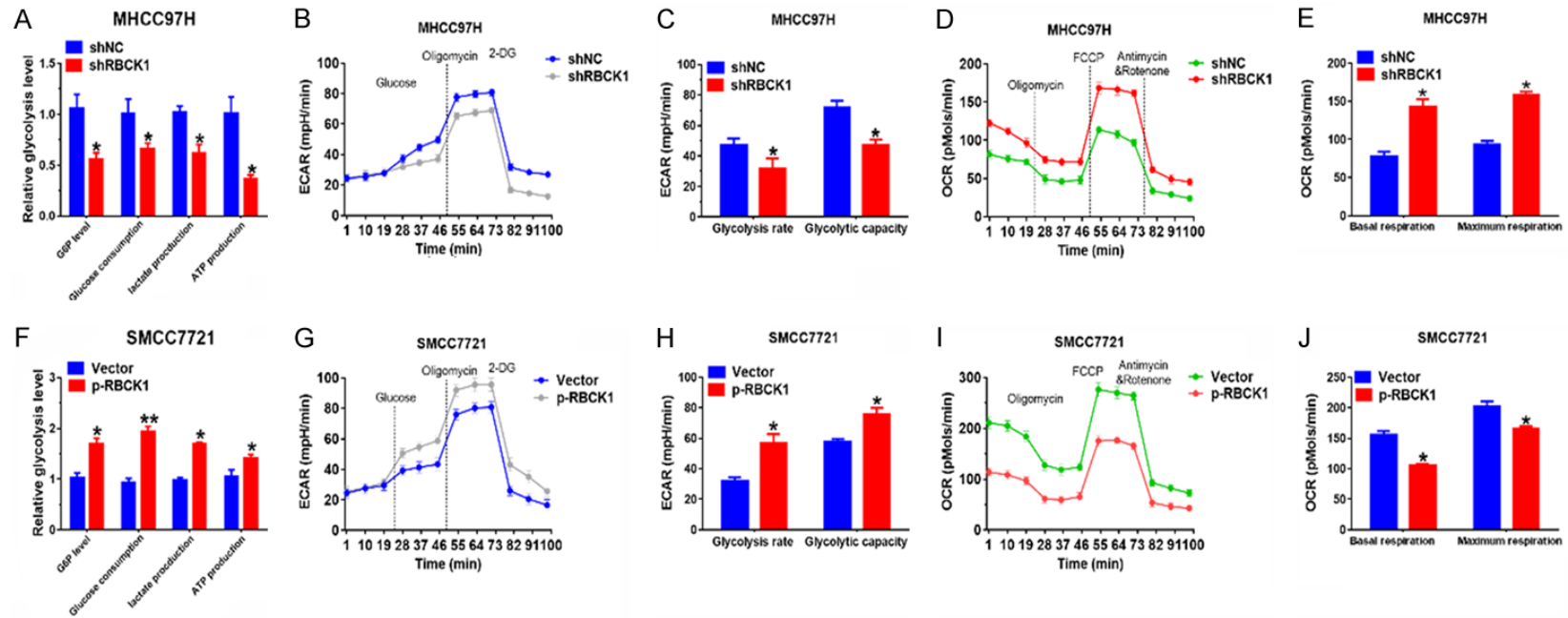
Figure S2. A. Cellular G6P levels, glucose consumption, lactate production, and ATP levels in SMCC7721/shRBCK1 cells. Three independent experiments were performed. *P<0.05. B and C. ECAR data showing the glycolytic rate and capacity in RBCK1-silenced SMCC7721 cells. D and E. OCR results showing the basal respiration and maximum respiration in RBCK1-silenced SMCC7721 cells. F. Cellular G6P levels, glucose consumption, lactate production, and ATP levels in SK-Hep-1/p-RBCK1 cells. G and H. ECAR data showing the glycolytic rate and capacity in RBCK1-overexpressing SK-Hep-1 cells. *P<0.05, **P<0.01. I and J. OCR results showing the basal respiration and maximum respiration in RBCK1-overexpressing SK-Hep-1 cells. *P<0.05.
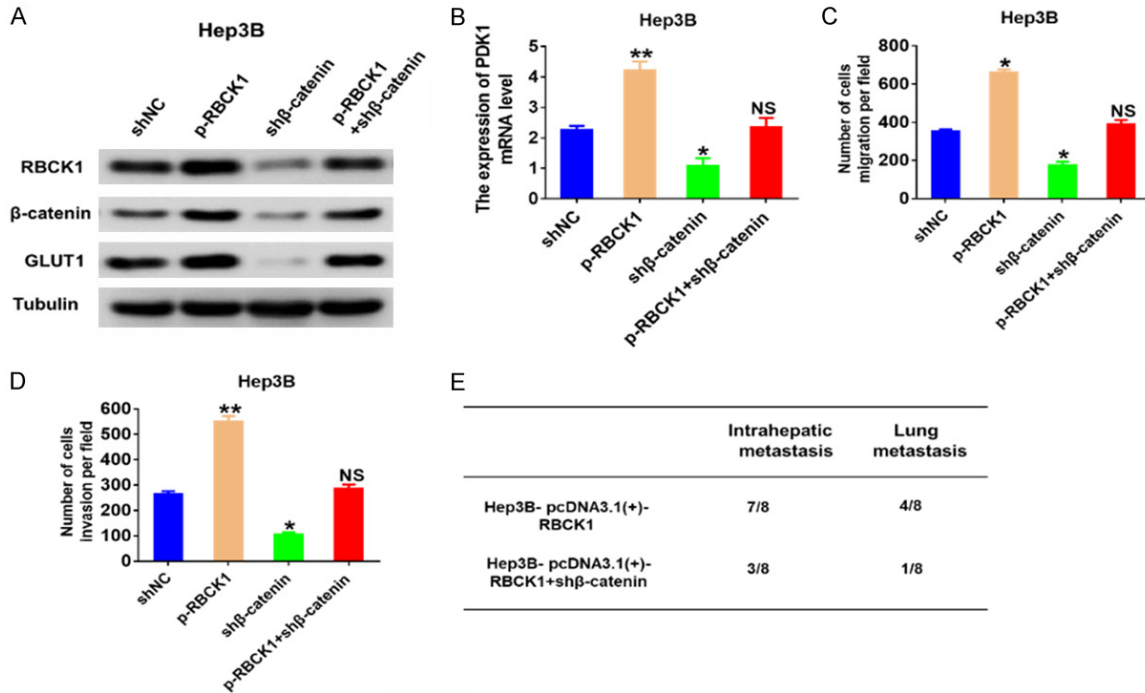
Figure S3. A and B. Western blotting and qRT-PCR showing the expression level of RBCK1, β-catenin and GLUT1 in RBCK1-overexpressing Hep3B cells transfected with shβ-catenin. Tubulin was a loading control. *P<0.05, **P<0.01. C and D. The quantification of Transwell assays in RBCK1-overexpressing Hep3B cells transfected with shβ-catenin. *P<0.05, **P<0.01. E. Quantification (left) of intrahepatic and lung metastases in the different groups of nude mice. n=8.
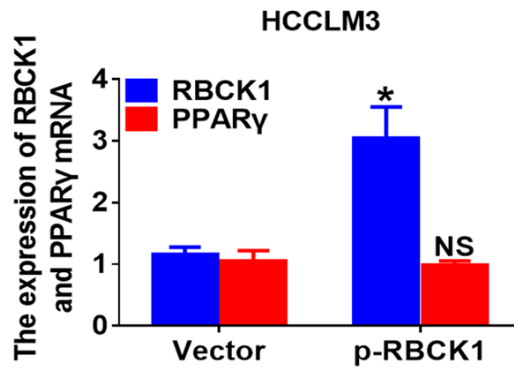
Figure S4. qRT-PCR showing expression levels of RBCK1 and PPARγ in RBCK1-overexpressed HCCLM3 cells.